channels. The use of X-ray crystallography and cryo-electron microscopy to define the structure of channels at atomic resolution provides a framework for achieving greater understanding of the mechanisms of ion channel function and malfunction due to disease-causing mutations. Combining a wide array of data from these various approaches makes possible the construction of detailed molecular models, which can be tested by further experiments, as well as by theoretical approaches such as molecular dynamics simulation.

X-Ray Crystallographic Analysis of Potassium Channel Structure Provides Insight Into Mechanisms of Channel Permeability and Selectivity

The first high-resolution X-ray crystallographic analysis of the molecular architecture of the pore region of an ion-selective channel was provided by Rod MacKinnon and his colleagues. To overcome the difficulties inherent in obtaining crystals of large integral membrane proteins, they initially focused on a non–voltage-gated K^+ channel, termed KcsA, from a bacterium. This channel is advantageous for crystallography as it can be expressed at high levels for purification, is relatively small, and has a simple transmembrane topology similar to that of the inward-rectifying K^+ channel in higher organisms, including mammals (Figure 8–11B).

The crystal structure of the KcsA protein provides several important insights into the mechanisms by which the channel facilitates the movement of K^+ ions across the hydrophobic lipid bilayer. The channel is made up of four identical subunits arranged symmetrically around a central pore (Figure 8–12A). Each subunit has two membrane-spanning α-helixes, an inner and outer helix. They are connected by the P-loop, which forms the selectivity filter of the channel. The amino acid sequence of these subunits is homologous to that of the S5-P-S6 region of vertebrate voltage-gated K^+ channels. The two α-helixes of each subunit tilt away from the central axis of the pore such that the structure resembles an inverted tepee (Figure 8–12B,C).

The four inner α-helixes from each of the subunits line the cytoplasmic end of the pore. At the intracellular mouth of the channel, these four helixes cross, forming a very narrow opening—the "smoke hole" of the tepee. Because this hole is too small to allow passage of K^+ ions, the crystal structure is presumed to represent the channel in the closed state. The inner helixes are homologous to the S6 membrane-spanning segment of voltage-gated K^+ channels (Figure 8–11A). At the extracellular end of the channel, the transmembrane helixes in each subunit are connected by a region consisting of three elements: (1) a chain of amino acids that surrounds the mouth of the channel (the turret region), (2) an abbreviated α-helix (the pore helix) approximately 10 amino acids in length that projects toward the central axis of the pore, and (3) a stretch of 5 amino acids near the C-terminal end of the P-region that forms the selectivity filter.

The shape and structure of the pore determine its ion-conducting properties. Both the inner and outer mouths of the pore are lined with acidic amino acids whose negative charges help attract cations from the bulk solution. Going from inside to outside, the pore consists of a medium-wide tunnel, 18 Å in length, which leads into a wider (10 Å diameter) spherical inner chamber. This chamber is lined predominantly by the side chains of hydrophobic amino acids. These relatively wide regions are followed by the very narrow selectivity filter, only 12 Å in length, which is rate-limiting for the passage of K^+ ions. A high K^+ ion throughput rate is ensured by the fact that the inner 28 Å of the pore, from the cytoplasmic entrance to the selectivity filter, lacks polar groups that could delay ion passage by binding and unbinding the ion (Figure 8–12C,D).

An ion passing from the polar solution through the nonpolar lipid bilayer encounters the least energetically favorable region in the middle of the bilayer. The large energy difference between these two regions for a K^+ ion is minimized by two details of channel structure. The inner chamber is filled with water, which provides a highly polar environment, and the pore helixes provide dipoles whose electronegative carboxyl ends point toward this inner chamber (Figure 8–12C).

The high energetic cost incurred as a K^+ ion sheds its waters of hydration is partially compensated by the presence of 20 electronegative oxygen atoms that line the walls of the selectivity filter and form favorable electrostatic interactions with the permeant ions. Each of the four subunits contributes four main-chain carbonyl oxygen atoms from the protein backbone and one side-chain hydroxyl oxygen atom to form a total of four binding sites for K^+ ions. Each bound K^+ ion is thus stabilized by interactions with a total of eight oxygen atoms, which lie in two planes above and below the bound cation. In this way, the channel is able to compensate for the loss of the K^+ ion's waters of hydration. The selectivity filter is stabilized at a critical width, such that it provides optimal electrostatic interactions with K^+ ions as they pass but is too wide for the smaller Na^+ ions to interact effectively with all eight oxygen atoms at any point along the length of the filter (Figure 8–12C).

In light of the extensive interactions between a K^+ ion and the channel, how does the KcsA channel

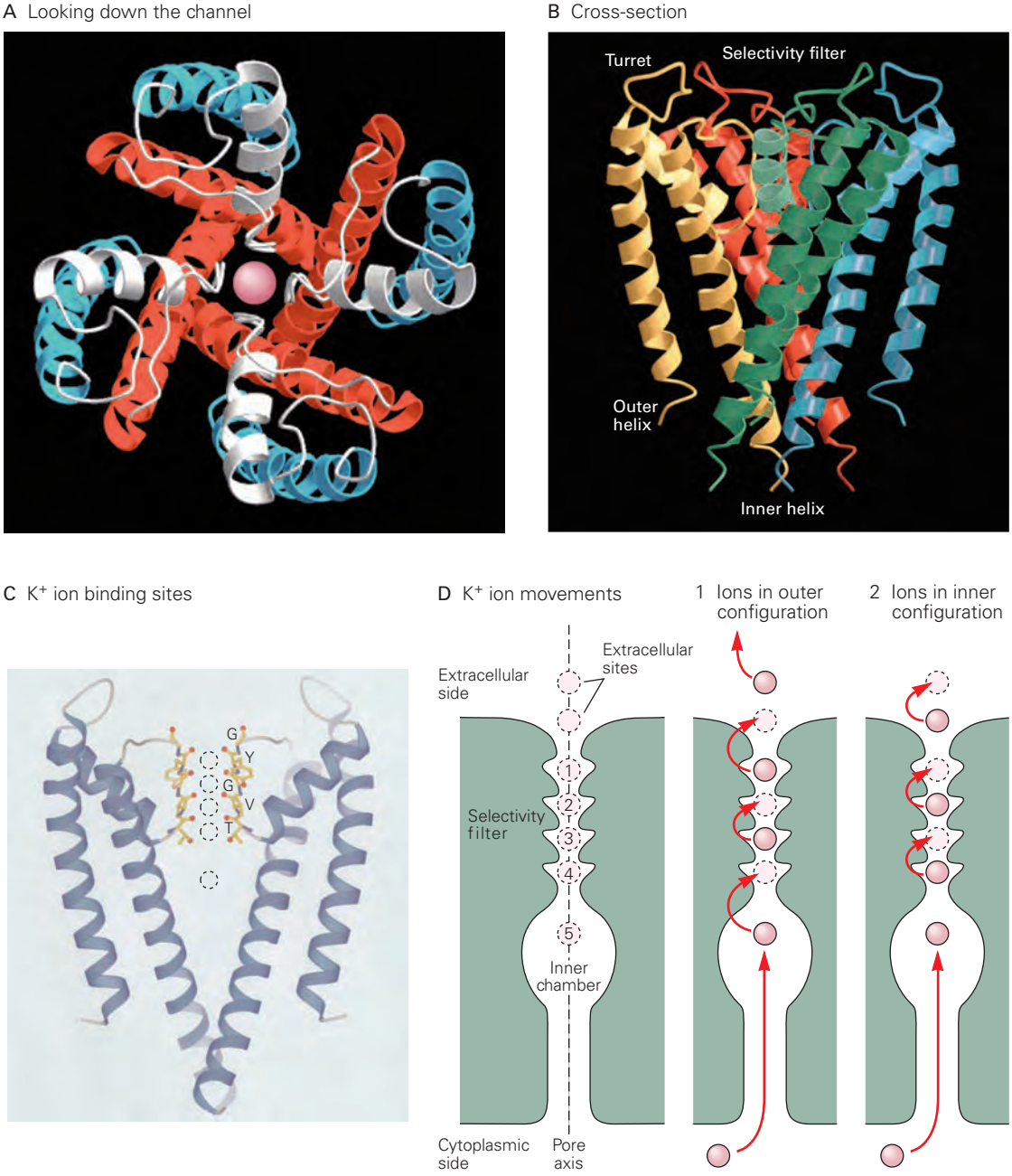

Figure 8–12 The X-ray crystal structure of a bacterial potassium channel. (Reproduced, with permission, from Doyle et al. 1998. Copyright © 1998 AAAS.)

A. The view is looking down the channel pore from outside the cell. Each of the four subunits of the KcsA K^+ channel contributes two membrane-spanning helixes, an outer helix (**blue**) and an inner helix (**red**). The P-region (**white**) lies near the extracellular surface of the channel pore and consists of a short α-helix (pore helix) and a loop that forms the selectivity filter of the channel. In the center of the pore is a K^+ ion (**pink**).

B. The channel is seen in a side view within a cross section of the membrane. The four subunits are shown in different colors.

C. Another view in the same orientation as in **part B** shows only two of the four subunits. The channel contains five K^+ binding sites (**dashed**). Four of the sites lie in the selectivity filter (**yellow**), while the fifth site lies in an inner chamber near the center of the channel. The four K^+ binding sites of the selectivity filter are formed by successive rings of oxygen atoms (**red**) from five amino acid residues per subunit. Four of the rings are formed by carbonyl oxygen atoms from the main chain backbone of four consecutive amino acid residues—glycine (**G**), tyrosine (**Y**), glycine (**G**), and valine (**V**). A fifth ring of oxygen near the internal end of the selectivity filter is formed by the side-chain hydroxyl oxygen of threonine (**T**). Each ring contains four oxygen atoms, one from each subunit. Only the oxygen atoms from two of the four subunits are shown in this view. (Reproduced, with permission, from Morais-Cabral et al. 2001. Copyright © 2001 Springer Nature.)

D. A view of K^+ ion permeation through the channel illustrates the sequence of changes in occupancy of the various K^+ binding sites. A pair of ions hops in concert between a pair of binding sites in the selectivity filter. In the initial state, the "outer configuration," a pair of ions is bound to sites 1 and 3. As an ion enters the inner mouth of the channel, the ion in the inner chamber jumps to occupy the innermost binding site of the selectivity filter (site 4). This causes the pair of ions in the outer configuration to hop outward, expelling an ion from the channel. The two ions now in the inner configuration (sites 2 and 4) can hop to binding sites 1 and 3, returning the channel to its initial state (the outer configuration), from which it can conduct a second K^+ ion. (Adapted, with permission, from Miller 2001. Copyright © 2001 Springer Nature.)

manage its high rate of conduction? Although the channel contains a total of five potential binding sites for K^+ ions, X-ray analysis shows that the channel can be occupied by at most three K^+ ions at any instant. One ion is normally present in the wide inner chamber, and two ions occupy two of the four binding sites within the selectivity filter (Figure 8–12D).

These structural data led to the following hypothesis. Because of electrostatic repulsion, two K^+ ions never simultaneously occupy adjacent binding sites within the selectivity filter; rather, a water molecule is always interposed between K^+ ions. During conduction, a pair of K^+ ions within the selectivity filter hop in tandem between pairs of binding sites. If only one ion were in the selectivity filter, it would be bound rather tightly, and the throughput rate for ion permeation would be compromised. But the mutual electrostatic repulsion between two K^+ ions occupying nearby sites ensures that the ions will linger only briefly, thus resulting in a high overall rate of K^+ conduction.

The form of the KcsA selectivity filter appears to be highly conserved among various types of mammalian voltage-gated K^+ channels. However, more recent studies by MacKinnon and colleagues have revealed how variations in geometric and surface charge features below the selectivity filter of this canonical pore can cause some voltage-gated K^+ channels to differ markedly in single-channel conductance and in affinity for various open channel blockers.

The snug fit between the K^+ channel selectivity filter and K^+ ions that helps explain the unusually high selectivity of these channels is not representative of all channel types. As we shall see in later chapters, in many channels pore diameters are significantly wider than the principal permeating ion, contributing to a lower degree of selectivity.

X-Ray Crystallographic Analysis of Voltage-Gated Potassium Channel Structures Provides Insight into Mechanisms of Channel Gating

As described earlier, the S4 segment of voltage-gated ion channels is thought to be the voltage sensor that detects changes in membrane potential. How do the positive charges in S4 move through the membrane electric field in response to a change in membrane potential? How is S4 movement coupled to gating? What is the relationship of the voltage-sensing region to the pore-forming region of the channel? What is the configuration of the open channel? Some answers to these questions have come from X-ray crystallographic analyses of mammalian voltage-gated K^+ channels, as well as from a number of studies using mutagenesis and other biophysical approaches. MacKinnon and colleagues studied the mammalian voltage-gated Kv1.2 K^+ channel, as well as a closely related chimera Kv1.2-Kv2.1, which yielded higher-resolution images.

Their analysis of X-ray crystal structures of the Kv1.2 channel and the Kv1.2-2.1 chimera showed that a K^+ channel subunit has two domains. The S1–S4 segments form a voltage-sensing domain at the periphery of the channel, whereas the S5-P–S6 segments form the pore domain at the central axis of the channel. The two domains are linked at their intracellular ends by the short S4–S5 coupling helix (Figure 8–13). The idea that the S1–S4 voltage sensor is a separate domain is supported by the fact that certain bacterial proteins contain S1–S4 domains but lack a pore domain. One such protein is a voltage-sensitive phosphatase, while another forms a voltage-gated proton channel. Conversely, the inward-rectifying K^+ channels (Figure 8–11B) have a high K^+ selectivity but are not directly gated by voltage because they lack the voltage sensor domain.

The crystal structures also help clarify what happens when the channel opens. Studies by Clay Armstrong in the 1960s suggested that a gate exists at the intracellular mouth of voltage-gated K^+ channels of higher organisms. He found that small organic cations such as tetraethylammonium (TEA) can enter and block the channel only when this internal gate is opened by depolarization. As described earlier, in the closed bacterial K^+ channels the four inner transmembrane helixes, which correspond to the S6 helixes in voltage-gated K^+ channels, meet at a tight bundle crossing at their cytoplasmic ends to form the closed gate of the channel (Figure 8–12). In contrast, the S6 helix of the Kv1.2–2.1 chimera is bent at a flexible three-amino-acid hinge (proline-valine-proline), causing the inner end of the helix to bend outward. This configuration results in an open channel conformation with an internal orifice that is dilated to 12 Å in diameter, wide enough to pass fully hydrated K^+ ions as well as larger cations such as TEA (Figures 8–13 and 8–14C). Once inside the channel lumen, TEA blocks K^+ permeation because it is too large to pass through the selectivity filter. It is not surprising that the Kv channel is in the open state, as there is no voltage gradient across the channel in the crystals. This is similar to the situation in a membrane that has been depolarized to 0 mV, a voltage at which the channels are normally open. This opening mechanism is likely to be a general one because the inner helixes of many K^+ channels in bacteria and higher organisms also have a flexible hinge at this position.

One long-standing question concerns the placement and movement of the gating charges on the S4

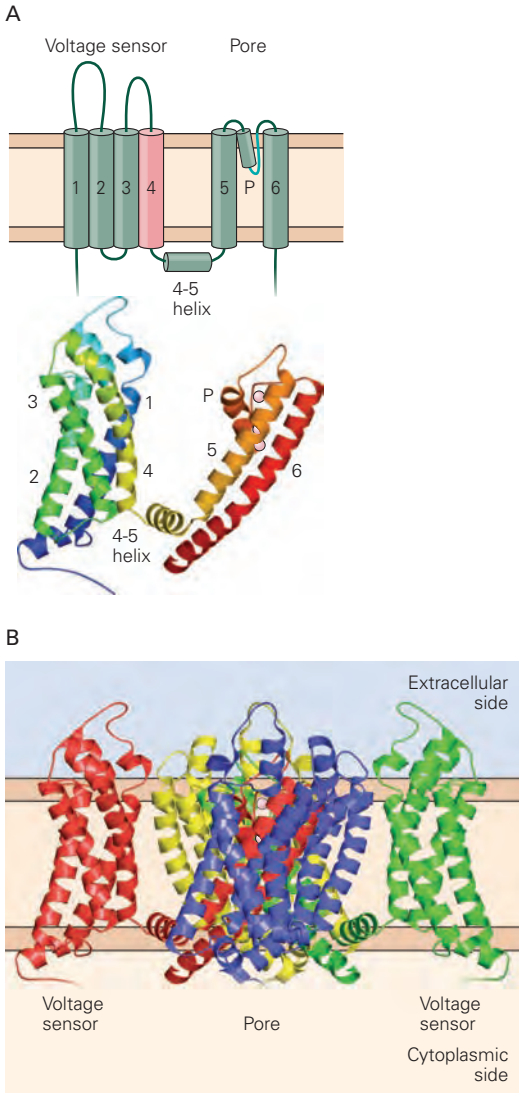

Figure 8–13 X-ray crystal structure of a voltage-gated potassium channel. (Adapted, with permission, from Long et al. 2007. Copyright © 2007 Springer Nature.)

A. *Top*: In addition to its six transmembrane α-helixes (**S1–S6**), a voltage-gated K^+ channel subunit contains a short α-helix (the **P** helix) that is part of the P-region selectivity filter, as well as an α-helix on the cytoplasmic side of the membrane that connects transmembrane helixes S4 and S5 (4–5 coupling helix). *Bottom*: An X-ray structural model of a single subunit shows the positions of the six membrane-spanning helixes, the P helix, and the 4–5 coupling helix. The S1–S4 voltage-sensing region and S5-P–S6 pore-forming regions are localized in separate domains. Two K^+ ions bound in the pore are shown in **pink**.

B. In this side view of the channel, each subunit is a different color. Subunit 6 (**red**) is in the same orientation as in **part A**.

segment voltage sensor. As mentioned earlier, movement of these charges within the plane of the membrane in response to changes in membrane potential is thought to couple membrane depolarization to channel gating. However, placement of charges within the hydrophobic membrane results in an unfavorable energy state, as discussed earlier for free ions in solutions. How do ion channels compensate for this unfavorable free energy?

The crystal structure provides some answers to this question. Mutagenesis studies indicate that four positively charged arginine residues in the external half of the S4 segment are likely to carry most of the gating charge. In the open state, the four positive charges face outward toward the extracellular side of the membrane, where they may undergo energetically favorable interactions with water or with the negatively charged head groups of the phospholipid bilayer. Positive charges on other S4 residues that lie more deeply within the lipid bilayer are stabilized by interactions with negatively charged acidic residues on the S1–S3 transmembrane helixes.

At present, a crystal structure for the closed state of the Kv1.2–Kv2.1 chimera is lacking. However, MacKinnon and colleagues have proposed a plausible model for voltage gating based on the structures of the open voltage-gated K^+ channel and the closed bacterial K^+ channel KcsA (Figure 8–14). According to this model, a negative voltage inside the cell exerts a force on the positively charged S4 helix that causes it to move inward by about 1.0 to 1.5 nm. As a result, the four positively charged S4 residues, which in the depolarized state face the external environment and sense the extracellular potential, now face the intracellular side of the membrane and sense the intracellular potential. In this manner, movement of each S4 segment will translocate 3 to 4 gating charges across the membrane electric field as the channel transitions between the closed and open states, for a total of 12 to 16 charges moved per tetrameric channel. This number is similar to the total gating charge movement determined from biophysical measurements (Chapter 10).

How are S4 movements coupled to the gate of the channel? According to the model, when the membrane voltage becomes negative, the resulting inward movement of the S4 segment exerts a downward force on the S4–S5 coupling helix. This helix, which lies roughly parallel to the membrane at its cytoplasmic surface, rests on the inner end of the S6 helix gate in the open state. As the S4–S5 helix moves downward, it acts as a lever, applying force to S6 and closing the gate. Thus, voltage-gating is thought to rely on the electromechanical coupling between the voltage-sensing domain and the

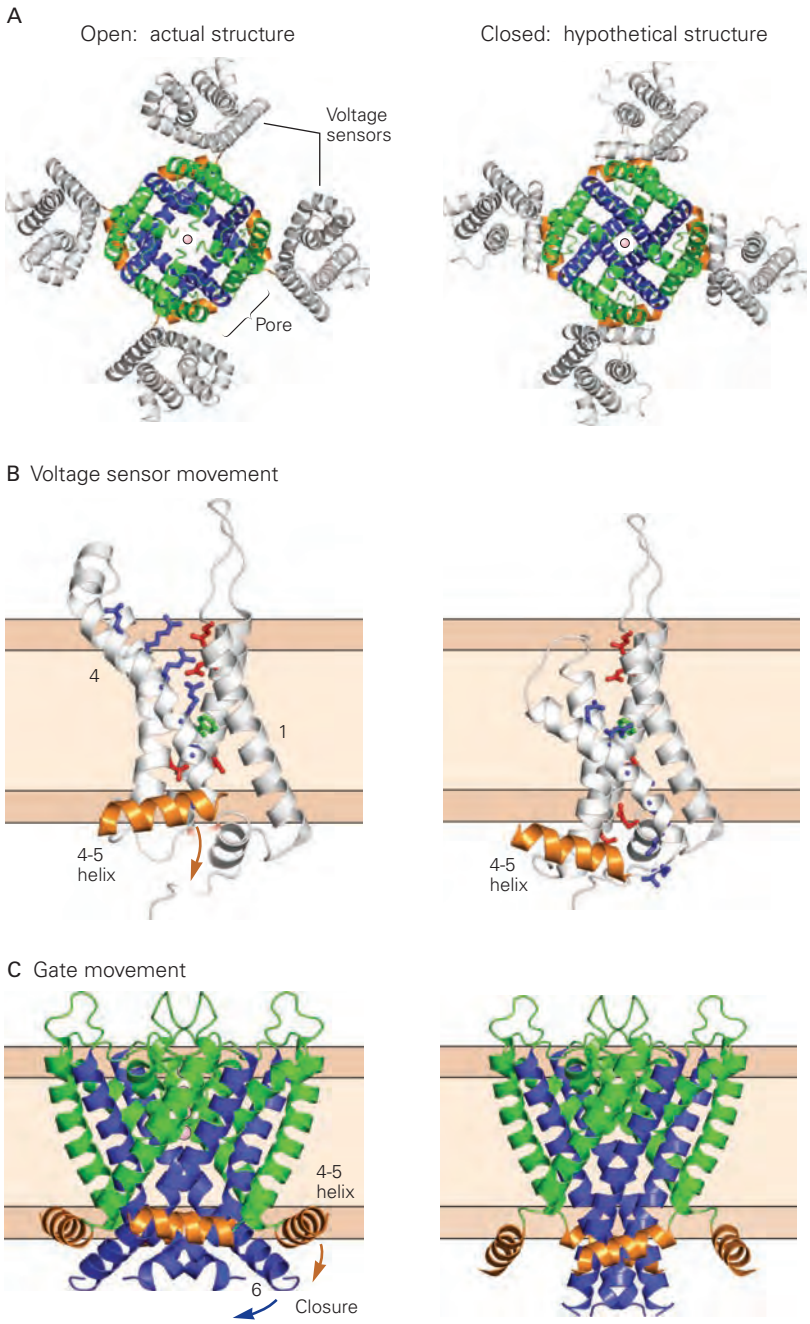

Figure 8–14 Model for voltage gating based on X-ray crystal structures of two potassium channels. In each part of the figure, the drawing on the *left* shows the actual structure of the open voltage-gated Kv1.2-2.1 chimera, while the drawing on the *right* shows the hypothetical structure of a closed voltage-gated K^+ channel, based in part on the structure of the pore region of the bacterial K^+ channel KcsA in the closed state. (Adapted, with permission, by Yuhang Chen from Long et al. 2007. Copyright © 2007 Springer Nature.)

A. A view looking down on the open and closed channel from outside the cell. The central pore is constricted in the closed state, preventing K^+ flow through the channel.

B. A view of the S1–S4 voltage-sensing domain from the side, parallel to the plane of the membrane. Positively charged residues in S4 are shown as **blue sticks**. In the open state, when the membrane is depolarized, four positive charges on the S4 helix are located in the external half of the membrane, facing the external solution. The positive charges in the interior of the membrane are stabilized by interactions with negatively charged residues in S1 and S2 (**red sticks**). In the closed state, when the membrane potential is negative, the S4 region moves inward so that its positive charges now lie in the inner half of the membrane. The inward movement of S4 causes the cytoplasmic S4–S5 coupling helix (**orange**) to move downward.

C. The putative conformational change in the channel pore upon voltage gating. A side view of the tetrameric S5-P–S6 pore region of the channel shows the S4–S5 coupling helix. Membrane repolarization causes the downward movement of the S4–S5 helix, applying force to the S6 inner helix of the pore (**blue**). This causes the S6 helix to bend at its pro-val-pro hinge, thereby closing the gate of the channel.

pore domain of the channel. Although this electromechanical coupling model provides a satisfying picture of how changes in membrane voltage lead to channel gating, a definitive answer to this key problem will require resolution of the structure of the closed state of a related voltage-gated mammalian K^+ channel.

Such a direct coupling between the sensing element of a channel (S4/S4–S5 linker) and the pore gate (S6) is found in most voltage-gated K^+ channels, as well as in voltage-gated Na^+ and Ca^{2+} channels. However, in many cases, the element of a channel that responds directly to the gating signal is not in direct contact with the channel gate, and instead, an allosteric mechanism propagates the response indirectly by more remote conformational changes. For example, in the voltage-gated K^+ channel Kv10, the S4–S5 linker is not in a position to act as a lever on S6. Rather, the inward movement of S4 in response to a negative potential closes the S6

gate indirectly, by laterally compressing the S5 helix, which is packed against the S6 helix. Additional cases of allosteric gating mechanisms are discussed later in the context of inactivation of voltage-gated Na^+ channels (Chapter 10) and activation of ligand-gated (Chapters 12 and 13) and mechanically gated channels (Chapter 18).

The Structural Basis of the Selective Permeability of Chloride Channels Reveals a Close Relation Between Channels and Transporters

Ions move across cell membranes by active transport by ion transporters or pumps, as well as by passive diffusion through ion channels. Ion transporters are distinguished from ion channels because (1) they use a source of energy to actively transport ions against their electrochemical gradients, and (2) they transport ions at rates much lower than ion channels, too low to support fast neuronal signaling. Nevertheless, some types of transporters and certain ion channels have similar structures, according to studies of the CLC family of proteins.

The CLC proteins expressed in vertebrates consist of a family of Cl^- channels and a closely related family of Cl^--H^+ cotransporters. Cotransporters use the electrochemical gradient of one ion to move another ion against its electrochemical gradient. The CLC Cl^--H^+ cotransporters, which are expressed in intracellular organelles, transfer two Cl^- ions across the membrane in exchange for one proton. This type of transporter is termed an ion exchanger.

The human voltage-gated ClC-1 channels are important for maintaining the resting potential in skeletal muscle (Chapter 57).

The crystal structures of the human ClC-1 channel and the homologous *E. coli* CLC exchangers have been determined by MacKinnon and colleagues. They found a close similarity in amino acid sequence to be reflected in a marked overall structural resemblance. Both types of CLC proteins consist of a homodimer composed of two identical subunits. Each subunit forms a separate ion pathway, and the two subunits function independently (Figure 8–15). The structures of the CLC proteins are quite different from those of K^+ channels. Unlike the pore of a K^+ channel, which is widest in the central region, each pore of the CLC protein has an hourglass profile. The neck of the hourglass, a tunnel 12 Å in length which forms the selectivity filter, is just wide enough to contain three fully dehydrated Cl^- ions.

Although the ion permeation pathways of the CLC proteins and the K^+ channel differ in significant respects, they have evolved four similar features that are critical to their function. First, their selectivity filters contain multiple sequential binding sites for the permeating ion. Multi-ion occupancy creates a metastable state that facilitates rapid ion passage. Second, the ion binding sites are formed by polar, partially charged atoms, not by fully ionized atoms. The resultant relatively weak binding energy ensures that the permeating ions do not become too tightly bound. Third, permeant ions are stabilized in the center of the membrane by the positively polarized ends of two α-helixes. Fourth, wide, water-filled vestibules at either end of the selectivity filter allow ions to approach the filter in a partially hydrated state. Thus although the K^+ channels and CLC proteins differ fundamentally in amino acid sequence and overall structure, strikingly

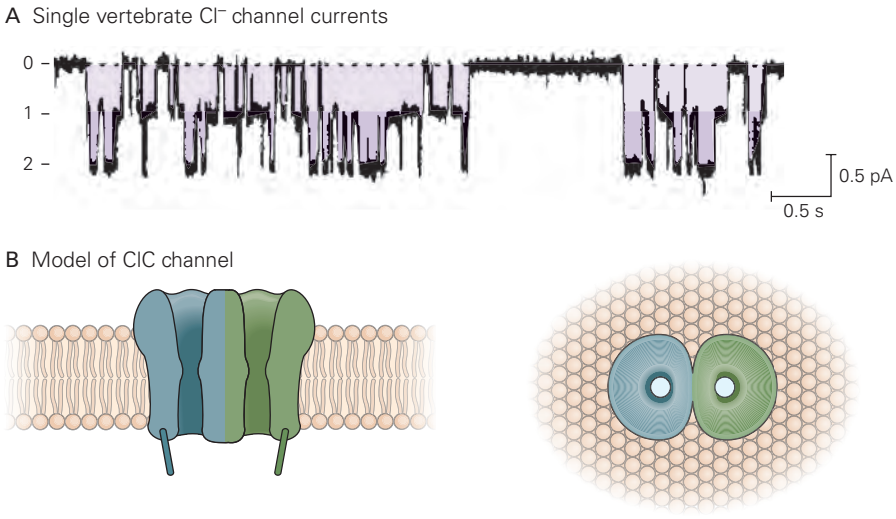

Figure 8–15 The vertebrate CLC family of chloride channels and transporters are double-barrel channels with two identical pores.

A. Recordings of current through a single vertebrate Cl^- channel show three levels of current: both pores closed (**0**), one pore open (**1**), and both pores open (**2**). (Adapted from Miller 1982.)

B. The channel is shown from the side (*left*) and looking down on the membrane from outside the cell (*right*). Each subunit contains its own ion transport pathway and gate. In addition, the dimer has a gate shared by both subunits (not shown).

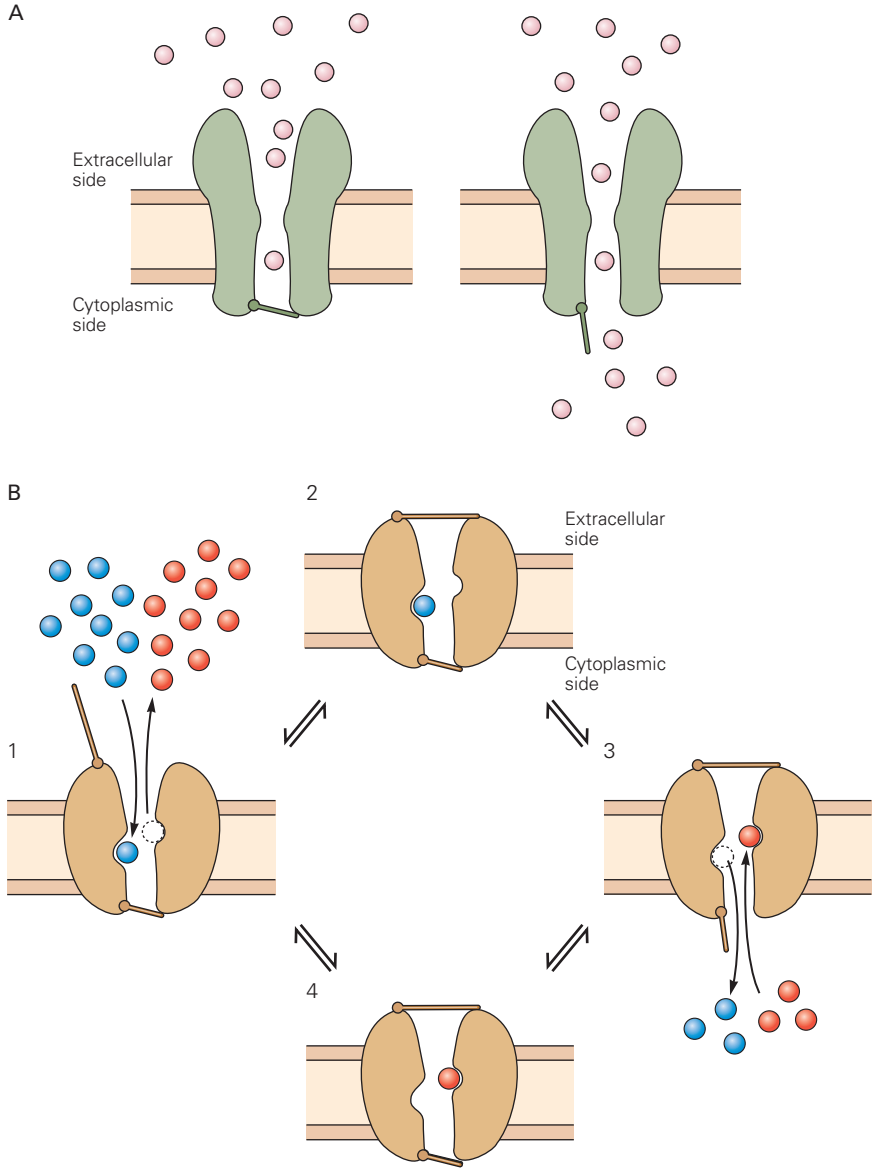

Figure 8–16 The functional difference between ion channels and transporters or pumps. (Adapted, with permission, from Gadsby 2004. Copyright © 2004 Springer Nature.)

A. Ion channels have a continuous aqueous pathway for ion conduction across the membrane. This pathway can be occluded by the closing of a gate.

B. Ion pumps and transporters have two gates in series that control ion flux. The gates are never open simultaneously, but both can close to trap one or more ions in the pore. The type of transporter illustrated here moves two different types of ions in opposite directions and is termed an *exchanger* or *antiporter*. Ion movement is tightly linked to a cycle of opening and closing of the two gates. When the external gate is open, one type of ion leaves while the other type enters the pore (**1**). This triggers a conformational change, causing the external gate to shut, thereby trapping the incoming ion (**2**). A second conformational change then causes the internal gate to open, allowing the trapped ion to leave and a new ion to enter (**3**). A further conformational change closes the internal gate, allowing the cycle to continue (**4**). With each cycle, one type of ion is transported from the outside to the inside of the cell, whereas the other type is transported from the inside to the outside of the cell. By coupling the movements of two or more ions, an exchanger can use the energy stored in the electrochemical gradient of one ion to actively transport another ion against its electrochemical gradient.

similar functional features have evolved in these two classes of membrane proteins that promote both a high degree of ion selectivity and efficient throughput. These features have been conserved with surprising fidelity from prokaryotes through humans.

More detailed structural studies will be needed to understand how some CLC proteins function as Cl^--H^+ exchangers whereas others act as conventional channels. Most exchangers and pumps, such as the Na^+-K^+ pump (Chapter 9), are thought to have two gates, one external and one internal, which are never open simultaneously. Instead, ion movements and gate movements are presumed to be part of a tightly coupled reaction cycle (Figure 8–16). CLC exchangers apparently have two gates that control Cl^- flux, coupled to the protonation-deprotonation cycle of a flexible glutamate residue in the selectivity filter that shuttles protons across the membrane. The resultant conformational changes enable transport of Cl^- against its concentration gradient, driven by the flux of H^+ ions down their electrochemical gradient. CLC channels are apparently built on a very similar structure as the transporters, but with modified gates and small structural changes in the ion transport pathway that allow much more rapid movement of Cl^- down its electrochemical gradient.

Highlights

1. Ions cross cell membranes through two main classes of integral membrane proteins—ion channels and ion pumps or transporters.
2. Ion channels act as catalysts for the passive flux of ions across the membrane. Channels have a central water-filled pore that substitutes for the polar environment on either side of the membrane. It allows the electrically charged ions to rapidly cross the nonpolar environment of the cell membrane, driven by the ion's electrochemical gradient.
3. Most ion channels are selectively permeable to certain ions. The portion of the channel pore called the selectivity filter determines which ions can penetrate based on the ion's charge, size, and physicochemical interactions with the amino acids that line the wall of the pore.
4. Ion channels have gates that open and close in response to different signals. In the open state, channels generate ionic currents that produce rapid voltage signals that carry information in the nervous system and in other excitable cells.
5. Most ion channels have three states: open, closed, and inactivated or desensitized. Transitioning between these states is termed gating. Depending on the type of channel, gating is controlled by various factors, including membrane voltage, ligand binding, mechanical force, phosphorylation state, and temperature.
6. The most common ion channels in nerve and muscle cells belong to three major gene superfamilies, the members of which are related by gene sequence homology and, in most cases, by functional properties.
7. Most ion channels are composed of multiple subunits. Combinatorial permutations of these subunits can generate a diverse array of channels with different functional properties. Post-transcriptional modifications generate additional diversity.
8. The various types of ion channels are differentially expressed in different types of neurons and different regions of neurons, contributing to the functional complexity and computational power of the nervous system. The expression patterns of some ion channels and transporters change during development and in response to changes in neuronal activity patterns.
9. The rich variety of ion channels in different types of neurons has stimulated intensive efforts to develop drugs that can activate or block specific channel types in nerve and muscle cells. Such drugs would, in principle, maximize therapeutic effectiveness with minimal side effects.
10. Structure-function and X-ray crystallographic studies of voltage-gated ion channels have provided key insights into the molecular and atomic-level details of K^+ channel conduction, selectivity, and gating. Recent technical advances in single-particle cryo-electron microscopy have led to rapid progress in studies of a wide range of ion channels.
11. Active transport, which is mediated by integral membrane proteins called transporters or pumps, enables ions to move across the membrane against their electrochemical gradient. The driving force that generates active ion fluxes comes either from chemical energy (the hydrolysis of ATP) or from the favorable electrochemical potential difference for a cotransported ion.
12. Most ion transporters and pumps do not provide a continuous pathway for ions. Rather, they undergo conformational changes for the different phases of the transport cycle, thereby providing alternating access of the molecule's central lumen to the two sides of the membrane. Because these conformational changes are relatively slow,

they are much less efficient than ion channels in mediating ion fluxes.

John D. Koester
Bruce P. Bean

Selected Reading

Hille B. 2001. *Ion Channels of Excitable Membranes,* 3rd ed. Sunderland, MA: Sinauer.

Isacoff EY, Jan LY, Minor DL. 2013. Conduits of life's spark: a perspective on ion channel research since the birth of *Neuron*. Neuron 80:658–674.

Jentsch TJ, Pusch M. 2018. CLC chloride channels and transporters: structure, function, physiology and disease. Physiol Rev 98:1493–1590.

Miller C. 1987. How ion channel proteins work. In: LK Kaczmarek, IB Levitan (eds). *Neuromodulation: The Biological Control of Neuronal Excitability,* pp. 39–63. New York: Oxford Univ. Press.

Yu FH, Yarov-Yarovoy V, Gutman GA, Catterall WA. 2005. Overview of molecular relationships in the voltage-gated ion channel superfamily. Pharmacol Rev 57:387–395.

References

Accardi A, Miller C. 2004. Secondary active transport mediated by a prokaryotic homologue of ClC Cl^- channels. Nature 427:803–807.

Alberts B, Bray D, Lewis J, Raff M, Roberts K, Watson JD. 1994. *Molecular Biology of the Cell,* 3rd ed. New York: Garland.

Armstrong CM. 1971. Interaction of tetraethylammonium ion derivatives with the potassium channels of giant axons. J Gen Physiol 58:413–437.

Basilio D, Noack K, Picollo A, Accardi A. 2014. Conformational changes required for H^+/Cl^- exchange mediated by a CLC transporter. Nat Struct Mol Biol 21:456–464.

Bayliss WM. 1918. *Principles of General Physiology,* 2nd ed., rev. New York: Longmans, Greene.

Boscardin E, Alijevic O, Hummler E, Frateschi S, Kellenberger S. 2016. The function and regulation of acid-sensing ion channels (ASICs) and the epithelial Na+ channel (ENaC): IUPHAR Review 19. Br J Pharmacol. 173:2671–2701.

Brücke E. 1843. Beiträge zur Lehre von der Diffusion tropfbarflüssiger Korper durch poröse Scheidenwände. Ann Phys Chem 58:77–94.

Coste B, Xiao B, Santos JS, et al. 2012. Piezo proteins are pore-forming subunits of mechanically activated channels. Nature 483:176–181.

Doyle DA, Cabral JM, Pfuetzner RA, et al. 1998. The structure of the potassium channel: molecular basis of K^+ conduction and selectivity. Science 280:69–77.

Eisenman G. 1962. Cation selective glass electrodes and their mode of operation. Biophys J 2:259–323. Suppl 2.

Enyedi P, Gabor G. 2010. Molecular background of leak K^+ currents: two-pore domain potassium channels. Physiol Rev 90:550–605.

Feng L, Campbell EB, MacKinnon R. 2012. Molecular mechanism of proton transport in CLC Cl^-/H^+ exchange transporters. Proc Natl Acad Sci U S A 109:11699–11704.

Gadsby DC. 2004. Ion transport: spot the difference. Nature 427:795–797.

Hamill OP, Marty A, Neher E, Sakmann B, Sigworth FJ. 1981. Improved patch-clamp techniques for high-resolution current recording from cells and cell-free membrane patches. Pflugers Arch 391:85–100.

Hansen SB. 2015. Lipid antagonism: the PIP2 paradigm of ligand-gated ion channels. Biochim Biophys Acta 1851:620–628.

Henderson R, Unwin PNT. 1975. Three-dimensional model of purple membrane obtained by electron microscopy. Nature 257:28–32.

Hille B. 1973. Potassium channels selective permeability to small cations. J Gen Physiol 61:669–686.

Hille B. 1984. *Ion Channels of Excitable Membranes,* Sunderland, MA: Sinauer.

Isom LL, DeJongh KS, Catterall WA. 1994. Auxiliary subunits of voltage-gated ion channels. Neuron 12:1183–1194.

Kaczmarek LK. 2013. Slack, slick, and sodium-activated potassium channels. ISRN Neurosci 2013:354262.

Katz B, Thesleff S. 1957. A study of the "desensitization" produced by acetylcholine at the motor end-plate. J Physiol (Lond) 138:63–80.

Kyte J, Doolittle RF. 1982. A simple method for displaying the hydropathic character of a protein. J Mol Biol 157:105–132.

Lau C, Hunter MJ, Stewart A, Perozo E, and Vandenberg JI. 2019. Never at rest: insights into the conformational dynamics of ion channels from cryo-electron microscopy. J Physiol 596:1107–1119.

Lewis AH, Cui AF, McDonald MF, Grandl J. 2017. Transduction of repetitive mechanical stimuli by Piezo1 and Piezo2 ion channels. Cell Rep 19:2572–2585.

Long SB, Tao X, Campbell EB, MacKinnon R. 2007. Atomic structure of a voltage-dependent K^+ channel in a lipid membrane-like environment. Nature 450:376–382.

Miller C. 1982. Open-state substructure of single chloride channels from *Torpedo electroplax*. Philos Trans R Soc Lond B Biol Sci 299:401–411.

Miller C (ed). 1986. *Ion Channel Reconstitution.* New York: Plenum.

Miller C. 2001. See potassium run. Nature 414:23–24.

Morais-Cabral JH, Zhou Y, MacKinnon R. 2001. Energetic optimization of ion conduction rate by the K^+ selectivity filter. Nature 414:37–42.

Moran Y, Barzilai MG, Liebeskind BJ, Zakon HH. 2015. Evolution of voltage-gated ion channels at the emergence of Metazoa. J Exp Biol 218:515–525.

Murata Y, Iwasaki H, Sasaki M, Inaba K, Okamura Y. 2005. Phosphoinositide phosphatase activity coupled to an intrinsic voltage sensor. Nature 435:1239–1243.